Sphingomyelin Interfacial Behavior: The Impact of Changing Acyl Chain Composition

Xin-Min Li, Janice M. Smaby, Maureen M. Momsen, Howard L. Brockman, and Rhoderick E. Brown*
The Hormel Institute, University of Minnesota, Austin, Minnesota 55912 USA

ABSTRACT Sphingomyelins (SMs) containing homogeneous acyl chains with 12, 14, 16, 18, 24, or 26 carbons were synthesized and characterized using an automated Langmuir-type film balance. Surface pressure was monitored as a function of lipid molecular area at constant temperatures between 10°C and 30°C. SM containing lauroyl (12:0) acyl chains displayed only liquid-expanded behavior. Increasing the length of the saturated acyl chain (e.g., 14:0, 16:0, or 18:0) resulted in liquid-expanded to condensed two-dimensional phase transitions at many temperatures in the 10–30°C range. Similar behavior was observed for SMs with lignoceroyl (24:0) or (cerotoyl) 26:0 acyl chains, but isotherms showed only condensed behavior at 10 and 15°C. Insights into the physico-mechanical in-plane interactions occurring within the different SM phases and accompanying changes in SM phase state were provided by analyzing the interfacial area compressibility moduli. At similar surface pressures, SM fluid phases were less compressible than those of phosphatidylcholines with similar chain structures. The area per molecule and compressibility of SM condensed phases depended upon the length of the saturated acyl chain and upon spreading temperature. Spreading of SMs with very long saturated acyl chains at temperatures 30–35° below T_m resulted in condensed films with lower in-plane compressibilities, but consistently larger cross-sectional molecular areas than the condensed phases achieved by spreading at temperatures only 10–20° below T_m. This behavior is discussed in terms of the enhancement of SM lateral aggregation by temperature reduction, a common approach used during domain isolation from biomembranes.

INTRODUCTION

Sphingomyelin (SM) is a phosphosphingolipid that has been the focus of intense research over the past few years due to its role as a metabolic reservoir of messenger signals that have an impact on processes such as programmed cell death and related events such as cellular stress, mitogenesis, and senescence. Aside from involvement in signaling processes, sphingomyelins and glycosylated sphingolipids (along with cholesterol) also have been implicated in the formation of functional microdomains or lipid rafts in cell membranes (Brown and Rose, 1992; Simons and Ikonen, 1997). The physical environment provided within these putative microdomains is thought to play a key role in the lateral localization of certain GPI-anchored proteins involved in cellular signaling events (Brown, 1998; Rietveld and Simons, 1998; Brown and London, 1998). Yet another protein sorting process that may involve sphingomyelin occurs in the Golgi complex. Here, the retention of resident versus nonresident proteins has been hypothesized to reflect the energetically favored lateral partitioning between thicker (cholesterol-enriched) or thinner (cholesterol-poor) regions of the membrane to better accommodate the nonpolar membrane-spanning dimensionality of different protein families (Bretscher and Munro, 1993).

Because of the important functional role(s) that have been attributed to SM and related sphingolipids, understanding the structural basis for their physico-chemical behavior takes on added significance. Like PC, SM has phosphocholine as its zwitterionic polar headgroup. Although SM and PC both have two long nonpolar hydrocarbon chains configured in rather similar ways, this is where the similarity ends. In PC, both hydrocarbon chains are ester-linked to a glycerol backbone, the *sn*-1 chain usually is saturated (with, e.g., palmitate or stearate), and the *sn*-2 chain usually contains one or more *cis* double bonds. In contrast, in SM, the sphingoid base serves the dual roles as both interfacial backbone and nonpolar hydrocarbon chain. The only true acyl chain is amide-linked. The structural features that may enable SM to provide a specialized membrane environment include 1) an abundance of long, saturated acyl chains that sometimes provide marked intramolecular chain-length asymmetry; and 2) interfacial functional groups that can donate and accept hydrogen bonds with neighboring lipids (Barenholz and Thompson, 1980; Boggs, 1987). While many studies have focused on the latter feature, especially in relation to interactions with sterols (e.g., Sankaram and Thompson, 1990; Bittman et al., 1994), only relatively

Received for publication 27 August 1999 and in final form 13 January 2000.

Address reprint requests to Dr. Rhoderick E. Brown, Hormel Institute, 801 16th Ave. NE, Austin, MN 55912. Tel.: 507-433-8804; Fax: 507-437-9606; E-mail: reb@maroon.tc.umn.edu.

Portions of this investigation were presented at the 41st Annual Meeting of the Biophysical Society held in New Orleans, LA (see Smaby et al., 1997b).

Abbreviations used: GPI, glycosylphosphatidylinositol; BSM, bovine brain sphingomyelin; ESM, egg yolk sphingomyelin; PC, diacyl-*sn*-glycero-3-phosphocholine 12:0 SM, *N*-dodecanoyl sphingosylphosphocholine; 14:0 SM, *N*-tetradecanoyl sphingosylphosphocholine; 16:0 SM, *N*-hexadecanoyl sphingosylphosphocholine; 18:0 SM, *N*-octadecanoyl sphingosylphosphocholine; 24:0 SM, *N*-tetracosanoyl sphingosylphosphocholine; 26:0 SM, *N*-26:0 sphingosylphosphocholine; 18:1 SM, *N*-cis-9-octadecenoyl sphingosylphosphocholine; 24:1 SM, *N-cis*-15-tetracosanoyl sphingosylphosphocholine.

0006-3495/00/04/1921/11 $2.00

recently has the importance of acyl chain length and saturation begun to be recognized as a key structural feature in SM's interactions with other lipids and in the resulting physical environment within localized regions of the membrane (e.g., Silvius, 1992; Silvius et al., 1996; Schroeder et al., 1994; Smaby et al., 1994, 1996; Ahmed et al., 1997). Despite the fact that saturated chains of differing lengths dominate the acyl composition of most naturally occurring SMs, the effect of changing acyl chain length on the physical behavior of SM remains rather poorly understood (e.g., Snyder and Freire, 1980; Maulik et al., 1986; Sripada et al., 1987; Bar et al., 1997; Ramstedt and Slotte, 1999).

Here, we show how changes in saturated acyl chain length affect the interfacial behavior of SM at various fixed temperatures using a Langmuir film balance. This approach provides a means to investigate the influence of acyl chain length in SMs over a range of molecular cross-sectional areas known to occur in membrane systems, while avoiding changes in lipid mesomorphic behavior and aggregation state that often occur in model bilayer systems as temperatures are varied across the liquid-crystalline to gel phase transition temperature. The results not only supply insights into the in-plane elastic interactions of different pure SMs, but also provide a foundation for understanding the physical environment produced when SMs mix with other membrane lipids.

MATERIALS AND METHODS

Sphingomyelin synthesis

Sphingomyelins with homogeneous acyl chains were produced by reacylation of lyso-SM with the desired fatty acyl residue as described previously (Smaby et al., 1996 and references therein). Briefly, the *N*-hydroxy succinimide ester of the desired fatty acid was prepared, recrystallized, and reacted with lyso-SM, which had been produced by acidic deacylation of ESM. The reacylation reaction was performed at 60°C under nitrogen for 6–8 h in the presence of the catalyst, *N*-ethyldiisopropylamine. After reacylation, SM was purified by flash column chromatography and crystallized from $CHCl_3/CH_3OH$ using −20°C acetone. Using the preceding approach, we prepared 12:0 SM, 14:0 SM, 16:0 SM, 18:0 SM, 24:0 SM, 26:0 SM, 18:1 SM, and 24:1 SM. SM purity and *N*-acyl homogeneity were confirmed by TLC and by capillary gas chromatography, respectively. Final stock concentrations determined by dry weight using a Cahn microbalance (model 4700) and by phosphate analysis (Bartlett, 1959), matched to within 4%.

Monolayer conditions

Stock solutions of SMs were prepared by dissolving lipids in either petroleum ether/-ethanol or hexane (Burdick Jackson Laboratories, Muskegon, MI)/ethanol (95:5). Solvent purity was verified by dipole potential measurements (Smaby and Brockman, 1991a). Water for the subphase buffer was purified by reverse osmosis, activated charcoal adsorption, and mixed-bed deionization, then passed through a Milli-Q UV Plus System (Millipore Corp., Bedford, MA), and filtered through a 0.22 μm Millipak 40 membrane. Subphase buffer (pH 6.6) consisting of 10 mM potassium phosphate, 100 mM NaCl, and 0.2% NaN_3 was stored under argon until use.

Surface pressure-molecular area-surface potential (π-A) isotherms were measured using a computer-controlled, Langmuir-type film balance, calibrated according to the equilibrium spreading pressures of known lipid standards (Momsen et al., 1990). Lipids were dissolved (51.67 μl aliquots) and spread in hexane/ethanol (95:5). Films were compressed at a rate of ≤4 Å^2/molecule/min after an initial delay period of 4 min. The subphase was maintained at fixed temperature using a thermostatted, circulating water bath. Dipole potentials were measured using a ^{210}Po ionizing electrode. The film balance was housed in an isolated laboratory supplied with clean air by a Bioclean Air Filtration system equipped with charcoal and HEPA filters. The trough was separately enclosed under humidified argon, cleaned with a seven-stage series filtration set-up consisting of an Alltech activated charcoal gas purifier, a LabClean filter, and a series of Balston disposable filters consisting of two adsorption (carbon) and three filter units (93% and 99.99% efficiency at 0.1 μm). Other technical features that contribute to isotherm reproducibility include automated lipid spreading via a modified HPLC autoinjector, automated surface cleaning by multiple barrier sweeps between runs, and highly accurate and reproducible setting of the subphase level by an automated aspirator (Brockman et al., 1980, 1984).

Analysis of isotherms

In keeping with recent proposals, we avoid using the term "liquid condensed" and instead use the term "condensed" to denote monolayers states in which the hydrocarbon chains are ordered (Kaganer et al., 1999). The "liquid expanded" state differs from the condensed state in that the chains are conformationally disordered. Monolayer phase transitions between the liquid-expanded and condensed states were identified from the second and third derivatives of surface pressure (π) with respect to molecular area (A) as previously described (Ali et al., 1998).

Monolayer compressibilities were obtained from π-A data using:

$$\mathbf{C}_s = (-1/A)(\mathrm{d}A/\mathrm{d}\pi) \quad (1)$$

where A is the area per molecule at the indicated surface pressure and π is the corresponding surface pressure (e.g., Davies and Rideal, 1963; Behroozi, 1996). To facilitate comparisons with elastic moduli of area compressibility determinations in bilayer systems (e.g., Evans and Needham, 1987; Needham and Nunn, 1990), we expressed our data in terms of the reciprocal of the surface compressional modulus ($\mathbf{C}_s^{-1}$). We used a 100-point sliding window that utilized every fourth point to calculate a $\mathbf{C}_s^{-1}$ value before advancing the window one point. Each $\mathbf{C}_s^{-1}$ versus average molecular area curve consisted of 200 $\mathbf{C}_s^{-1}$ values obtained at equally spaced molecular areas along the π-A isotherms.

In earlier reports in which the π-$\mathbf{C}_s^{-1}$ behavior of various pure GalCers, SMs, PCs, or PC-cholesterol mixtures were investigated (Smaby et al., 1996, 1997), we discussed the limitations associated with experimentally derived $\mathbf{C}_s^{-1}$ values obtained at high surface pressures (>30–35 mN/m). $\mathbf{C}_s^{-1}$ values determined directly from experimental π-A isotherms display maxima below monolayer collapse rather than continuing to increase hyperbolically until film collapse. $\mathbf{C}_s^{-1}$ maxima generally occur at surface pressures >35 mN/m, but this depends upon the lipid or lipid mixture under study. The highly reproducible $\mathbf{C}_s^{-1}$ maxima may indicate precollapse behavior linked to intrinsic experimental factors (e.g., trough composition and/or design) or may also reflect a decrease in lipid film stability at high pressures. Analogously, the dipole potential (ΔV) versus inverse area behavior ($1/A$) of various liquid-expanded lipids reportedly is linear up to surface pressures where the second derivative of the π-A isotherms ($d^2\pi/dA^2$) goes from positive to negative values (π_d) (Smaby and Brockman, 1990). The linearity indicates a lack of significant dipole reorientation over the range of surface pressures leading up to π_d and typically encompasses 80–90% of the π-A data for liquid-expanded films. Hence, to model the $\mathbf{C}_s^{-1}$ data at high surface pressures, the experimentally

TABLE 1 Lipid interfacial elastic moduli of area compressibility at surface pressures of 30 mN/m

SM Species	Temp. (°C)	Phase State*	Molecular Area (Å^2)	$\mathbf{C}_s^{-1}$ (mN/m)†	SM Species	Temp. (°C)	Phase State*	Molecular Area (Å^2)	$\mathbf{C}_s^{-1}$ (mN/m)†
12:0 SM	10	L	52.3	128	18:1 SM	10	L	58.8	149
	15	L	54.1	125		15	L	58.6	141
	20	L	55.0	128		20	L	59.4	143
	24	L	56.9	130		24	L	60.3	146
	30	L	57.4	126		30	L	61.5	140
14:0 SM	10	M	46.9	150	24:0 SM	10	C	50.1	433
	15	M	51.3	77		15	C	49.4	266
	20	M	53.3	104		20	M	46.4	200
	24	L	56.3	130		24	M	46.9	187
	30	L	57.0	136		30	M	47.7	152
16:0 SM	10	C	46.3	351	26:0 SM	10	C	49.6	454
	15	C	45.9	326		15	C	48.6	353
	20	M	45.7	264		20	M	46.2	184
	24	M	47.4	196		24	M	46.0	165
	30	M	52.5	82		30	M	46.5	143
18:0 SM	10	C	48.0	359	24:1 SM	10	M	50.5	70
	15	C	47.6	316		15	M	54.6	56
	20	M	47.2	301		20	M	58.8	73
	24	M	47.1	279		24	M	59.6	97
	30	M	48.6	153		30	M	60.7	111

*Phase state: L denotes liquid-expanded (chain-disordered); C denotes condensed (chain-ordered); M denotes mixture of liquid-expanded and condensed states.

†Exptl. values were calculated as described in the Materials and Methods.

obtained π-A isotherms were fit using Film Fit (Creative Tension, Inc., Austin, MN) to the following osmotic-based monolayer equation of state:

$$\pi = (qkT/\omega_1)\ln[(1/f_1)[1 + \omega_1/(A_\pi - \omega_0)]] \qquad (2)$$

where k is Boltzmann's constant, ω_1 is the cross-sectional area of an interfacial water molecule (9.65 Å^2) and ω_0 is the cross-sectional area of dehydrated lipid, f_1 is the activity coefficient of interfacial water, and A_π is the total surface area divided by the number of lipid molecules present at a given surface pressure (Smaby and Brockman, 1992; Feng et al., 1994). The scaling parameter q correlates to f_1 and is not unique, but does provide a better fit of the data because it allows for higher-order terms involving the activity coefficient (Smaby and Brockman, 1991b; Feng et al., 1994). Using Eq. 2 as described previously (e.g., Ali et al., 1998), fitted π-A isotherms were generated that provided extrapolated π-A data at high π (approaching film collapse). Modeled $\mathbf{C}_s^{-1}$ values could then be determined from the extrapolated high-pressure data ($\pi \geq 30$ mN/m). For comparison with $\mathbf{C}_s^{-1}$ values calculated directly from experimental data, the modeled $\mathbf{C}_s^{-1}$ values are also presented in Tables 1 and 2. Data shown in the figures are experimental and were generated directly without fitting to Eq. 2.

RESULTS

16:0 SM and 18:0 SM

A hallmark of natural sphingomyelin is its long saturated acyl chain. While palmitate (16:0) and stearate (18:0) account for the majority of the acyl chains of egg yolk and BSM, respectively, much longer acyl residues (22:0, 23:0, and 24:0) predominate in milk and erythrocyte SM. In most earlier monolayer studies of SMs, investigations were focused on egg yolk or BSM, or on their respective major species containing palmitoyl (16:0) or stearoyl (18:0) acyl chains, and were confined to a single temperature. Although characterization of the surface pressure versus molecular cross-sectional area (π-A) isotherms was achieved, little or no attention was directed to the in-plane elastic interactions (Yedgar et al., 1982; Lund-Katz et al., 1988; Gronberg et al., 1991; Bittman et al., 1994; Smaby et al., 1994). As recently discussed, characterization of the interfacial elastic moduli of area compressibility ($\mathbf{C}_s^{-1}$) as a function of surface pressure or cross-sectional molecular area (A) provides valuable insights into lipid in-plane elastic interactions (Smaby et al., 1996; 1997a; Ali et al., 1998). These insights

TABLE 2 Interfacial elastic moduli of area compressibility (experimental versus fitted values at 30 mN/m)

Lipid	$\mathbf{C}_s^{-1}$ (mN/m) Exptl.*	$\mathbf{C}_s^{-1}$ (mN/m) Modeled†
14:0 SM	130	129
di-14:0 PC	110	118
18:0–10:0 PC	85	86
12:0 SM	130	129
18:1$^{\Delta 9(c)}$ SM	145	144
16:0–18:1$^{\Delta 9(c)}$ PC	123	123
18:0–18:1$^{\Delta 9(c)}$ PC	123	122

*Obtained from the experimental surface pressure versus molecular area isotherms by using the inverse of Eq. 1 (see Methods).

†Obtained by fitting the experimental surface pressure versus molecular area isotherms using Eq. 2 and then applying the inverse of Eq. 1 to the resulting fitted isotherms. Values for di-14:0 PC, 18:0–10:0 PC, 16:0–18:1$^{\Delta 9(c)}$ PC, and 18:0–18:1$^{\Delta 9(c)}$ PC are taken from Smaby et al. (1997a) and those for 18:1$^{\Delta 9(c)}$ SM appear in Smaby et al. (1996). All values pertain to liquid-expanded conditions at 24°C.

can be obtained over a broader range of phase state conditions and/or lipid mixing compositions than by complementary approaches such as micropipette aspiration, which requires stable bilayer vesicles (for additional details, see Smaby et al., 1996).

The π-A (*panel A*) and the $\mathbf{C}_s^{-1}$-A (*panel B*) behaviors of SMs with 16:0 and 18:0 acyl chains at various fixed temperatures in the range of 10–30°C are shown in Figs. 1 and 2, respectively. Two-dimensional phase transitions of a liquid-expanded (chain-disordered) to condensed (chain-ordered) nature are observed at many temperatures. This observation is consistent with the results of earlier studies carried out at a single temperature (e.g., Yedgar et al., 1982; Lund-Katz et al., 1988; Gronberg et al., 1991; Bittman et al., 1994; Smaby et al., 1994). The sharpness of the two-dimensional transition clearly depends on the homogeneity of the acyl composition in the SMs (Smaby et al., 1996). From Figs. 1 *A* and 2 *A* it is evident that the lower the temperature, then the lower the surface pressure (and larger the molecular area) that are observed at the onset of the two-dimensional phase transition. Dramatic drops in the $\mathbf{C}_s^{-1}$ values are observed across the phase transition regions

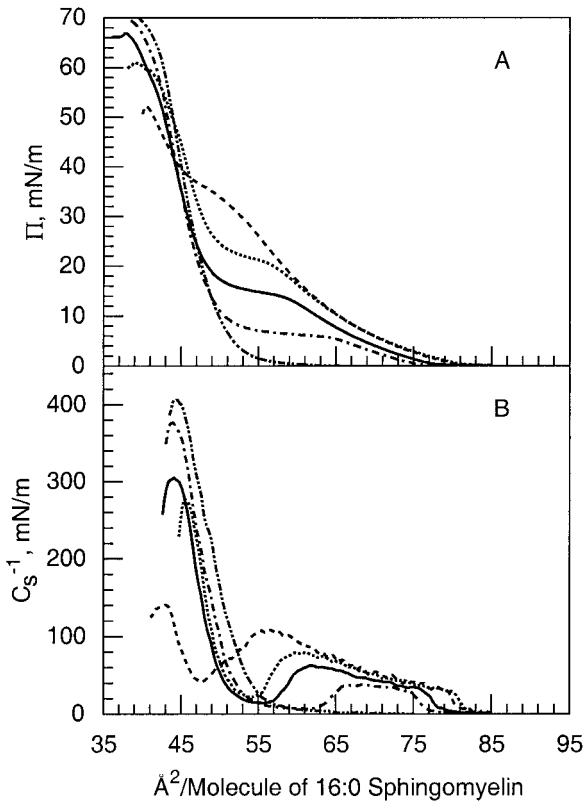

FIGURE 1 16:0 SM monolayers. Data were collected using an automated Langmuir-type film balance (see Methods). Traces at 10°C are indicated by (– · · –); at 15°C by (– · – ·); at 20°C by (——); at 24°C by (· · ·); and at 30°C by (– – –). (*A*) Surface pressure versus average cross-sectional molecular area (π-A). (*B*) Interfacial elastic modulus of area compressibility ($\mathbf{C}_s^{-1}$) versus average molecular area.

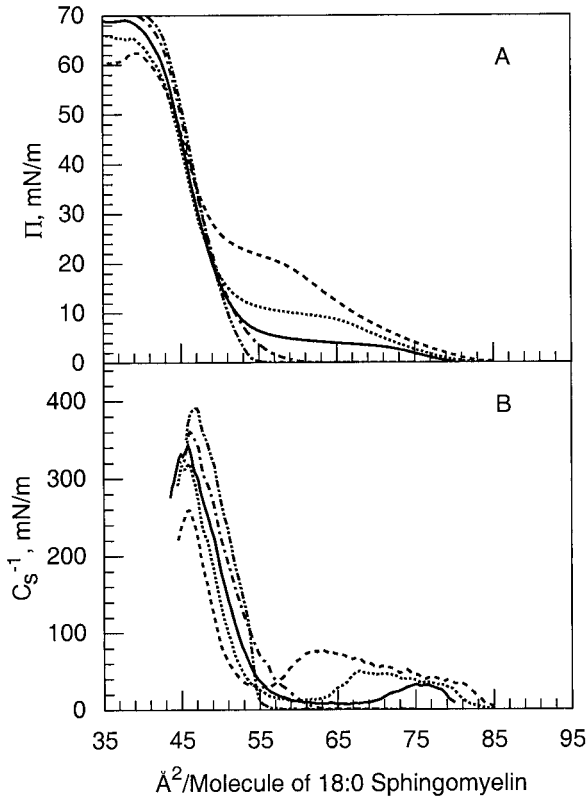

FIGURE 2 18:0 SM monolayers. (*A*) Surface pressure versus average cross-sectional molecular area (π-A). (*B*) Interfacial elastic modulus of area compressibility ($\mathbf{C}_s^{-1}$) versus average molecular area (other details same as in Fig. 1 legend).

of 16:0 SM and 18:0 SM at several temperatures in the 10–30°C range. As pointed out previously (Smaby et al., 1996; Ali et al., 1998), the sharp decline in the $\mathbf{C}_s^{-1}$ values upon entering the transition region reflects the difference in the partial molar area within the co-existing liquid-expanded (chain-disordered) and condensed (chain-ordered) phases (Phillips et al., 1975; Nagle and Scott, 1978; Mouritsen et al., 1989; Fornés and Procopio, 1995). Upon completion of the two-dimensional phase transition, much higher $\mathbf{C}_s^{-1}$ values characteristic of condensed (i.e., gel phase-like) behavior are observed.

12:0 SM and 14:0 SM

To determine the effect of shortening the *N*-linked acyl chain of SM, investigations were carried out with 12:0 SM and 14:0 SM. As can be seen in Fig. 3, liquid-expanded behavior, i.e., fluid phase, is observed for 12:0 SM at all temperatures in the 10–30°C range without any indication of two-dimensional phase transitions. In contrast, for 14:0 SM two-dimensional phase transitions occur at increasingly high surface pressures (and smaller molecular areas) at 10, 15, 20, and 24°C, respectively (Fig. 4 *A*). These transitions

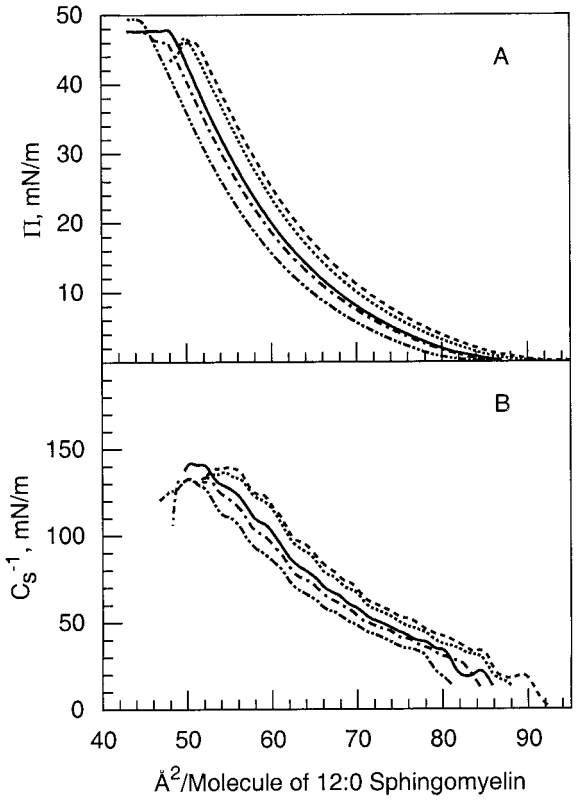

FIGURE 3 12:0 SM monolayers. (*A*) Surface pressure versus average cross-sectional molecular area (π-*A*). (*B*) Interfacial elastic modulus of area compressibility ($\mathbf{C}_s^{-1}$) versus average molecular area (other details same as in Fig. 1 legend).

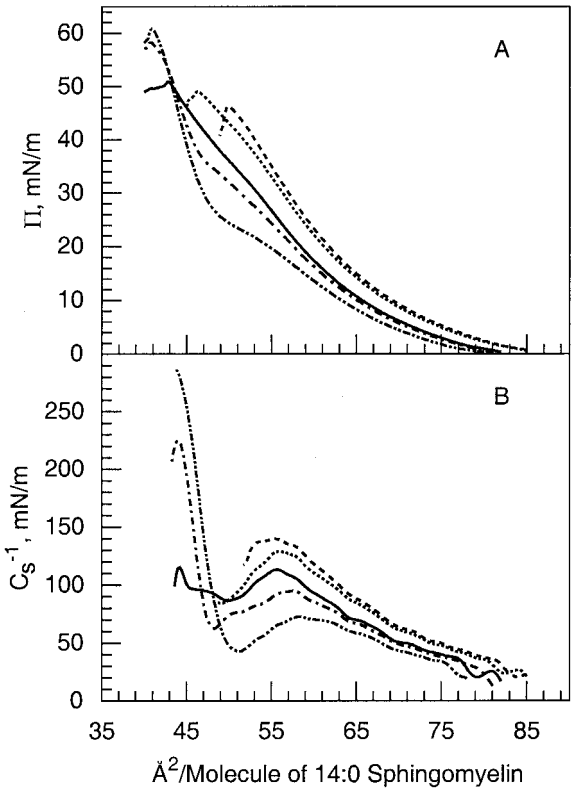

FIGURE 4 14:0 SM monolayers. (*A*) Surface pressure versus average cross-sectional molecular area (π-*A*). (*B*) Interfacial elastic modulus of area compressibility ($\mathbf{C}_s^{-1}$) versus average molecular area. (other details same as in Fig. 1 legend).

are especially apparent in the $\mathbf{C}_s^{-1}$-*A* plots (Fig. 4 *B*). Only liquid-expanded behavior, i.e., chain-disordered, was observed at 30°C. At high surface pressures such as those that mimic membrane-like conditions (for reviews, see Marsh, 1996; MacDonald, 1996), the experimental $\mathbf{C}_s^{-1}$ values for fluid phase 12:0 SM were consistently lower than those of 14:0 SM (e.g., at π = 30 mN/m, $\mathbf{C}_s^{-1}$ = 125 −130 mN/m range for 12:0 SM versus 135 mN/m for 14:0 SM; Tables 1 and 2).

24:0 SM and 26:0 SM

To determine the effect of lengthening the *N*-linked acyl chain, 24:0 SM and 26:0 SM were investigated. Because the sphingoid base is fixed in length and structurally equivalent to a 13.5 carbon, saturated *sn*-1 acyl chain of a phosphoglyceride, acylation of SM with 24:0 or 26:0 acyl chains results in marked chain-length asymmetry within the molecules. The π-*A* and $\mathbf{C}_s^{-1}$-*A* isotherms are shown for 24:0 SM and for 26:0 SM at 10, 15, 20, 24, and 30°C in Figs. 5 and 6, respectively. Both of these SMs show two-dimensional phase transitions at increasingly higher surface pressures (and smaller molecular areas) at temperatures of 20, 24, and 30°C. Thus, despite having one very long saturated chain (e.g., 24:0 or 26:0), two-dimensional phase transitions persist over a similar temperature range (20–30°C) as for much less asymmetric species, i.e., 18:0 SM. This observation is analogous to the thermotropic behavior reported in SM bilayers where lengthening the saturated acyl chain has only a moderate effect on elevating the major enthalpic transition (for review, see Koynova and Caffrey, 1995).

The isotherms also provide evidence for two differing condensed phases, i.e., chain-ordered, gel-like states. When 24:0 SM or 26:0 SM was spread at temperatures only 10–20° below T_m (e.g., at 20, 24, and 30°C), two-dimensional phase transitions were evident upon barrier compression. When these same lipids were spread at temperatures 30–35° below T_m, no barrier-dependent two-dimensional phase transition was evident. Interestingly, however, the resulting condensed state was characterized by consistently larger average molecular areas (at equivalent surface pressures) but higher $\mathbf{C}_s^{-1}$ values than occurred at the warmer temperatures when the condensed phase was produced by barrier compression. The higher $\mathbf{C}_s^{-1}$ values indicate a less compressible packing state with reduced in-plane elasticity despite the slightly larger average cross-sectional molecular area.

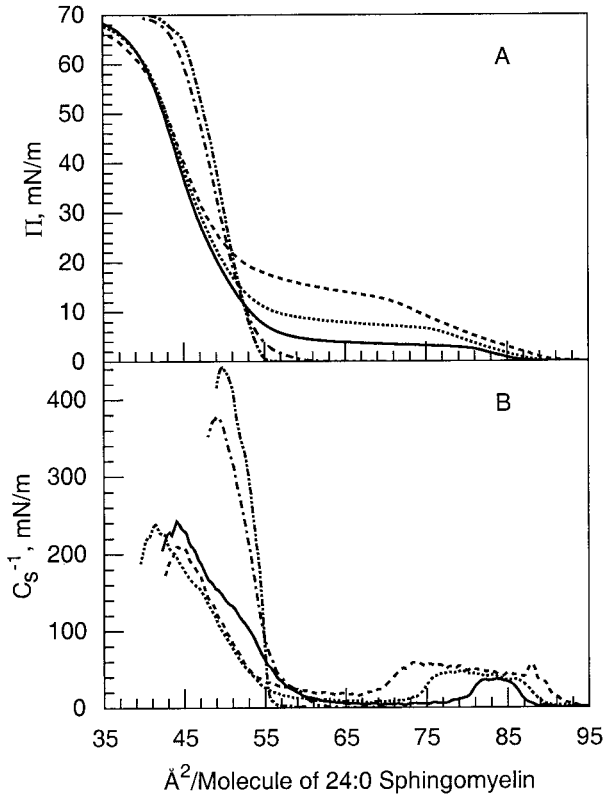

FIGURE 5 24:0 SM monolayers. (*A*) Surface pressure versus average cross-sectional molecular area (π-*A*). (*B*) Interfacial elastic modulus of area compressibility ($\mathbf{C}_s^{-1}$) versus average molecular area (other details same as in Fig. 1 legend).

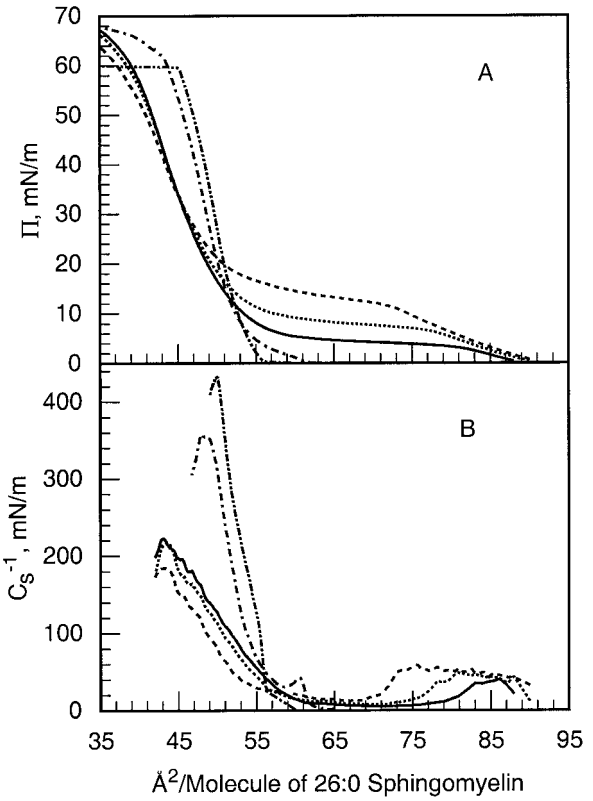

FIGURE 6 26:0 SM monolayers. (*A*) Surface pressure versus average cross-sectional molecular area (π-*A*). (*B*) Interfacial elastic modulus of area compressibility ($\mathbf{C}_s^{-1}$) versus average molecular area (other details same as in Fig. 1 legend).

18:1 SM and 24:1 SM

To compare the effect of "fluidizing" SM by having a *cis* double bond in the middle of a long acyl chain (e.g., 18:1$^{\Delta 9}$) versus having a short, saturated chain (e.g., 12:0), we investigated the interfacial behavior of 18:1 SM (Fig. 7). Liquid-expanded behavior was observed at all temperatures in the 10–30°C range. To compare the in-plane elasticity under membrane-like conditions, we determined the $\mathbf{C}_s^{-1}$ values at 30 mN/m. Although uncertainty exists as to the exact surface pressure value that places monolayers in equilibrium with bilayers (e.g., see Marsh, 1996; MacDonald, 1996; Feng, 1999), it is clear that this surface pressure value is relatively high ($\pi \geq 30$ mN/m). Interestingly, the $\mathbf{C}_s^{-1}$ values for 18:1 SM at 30 mN/m all were consistently higher than those of 12:0 SM and in the 140–145 mN/m range regardless of temperature (Tables 1 and 2). The behavior probably reflects a slight increase in van der Waals attractive forces due to a lengthening of the acyl chain despite the *cis* double bond being near the middle of the chain. A similar pattern of behavior was observed previously for the $\mathbf{C}_s^{-1}$ values of di-14:0 PC and 16:0–18:1 PC (Smaby et al., 1997a; Ali et al., 1998).

In naturally occurring SM the most common acyl monounsaturation occurs via a *cis* double bond at carbon 15 of a 24-carbon acyl chain. Despite having the *cis* double bond in the middle region of the acyl chain, 24:1 SM still exhibits a two-dimensional phase transition. In fact, the two-dimensional phase behavior resembles certain aspects of 14:0 SM behavior in that fluid phase behavior occurs at all surface pressures at 30°C, and two-dimensional phase transitions are observed at 24, 20, 15, and 10°C (Fig. 8). However, as shown in Table 1, at 30 mN/m the in-plane elasticity of the fluid phase state for 24:1 SM (at 30°C) is greater ($\mathbf{C}_s^{-1}$ = 111 mN/m) compared to that of 14:0 SM ($\mathbf{C}_s^{-1}$ = 135 mN/m) or to that of 18:1 SM ($\mathbf{C}_s^{-1}$ = 140 mN/m).

DISCUSSION

Previous monolayer studies of SMs have focused primarily on species with 16- or 18-carbon acyl chains, and/or have been limited to single temperatures (e.g., Yedgar et al., 1982; Lund-Katz et. al., 1988; Gronberg et al., 1991; Smaby et al., 1994; 1996; Bittman et al., 1994). Yet, recent studies suggest that other membrane lipids (e.g., PCs and cholesterol) mix differently with simple sphingolipids that lack hydrocarbon chain-length asymmetry compared to those with a high degree of hydrocarbon chain-length mismatch (e.g., 24:0 SM) (Bar et al., 1997; Ramstedt and Slotte,

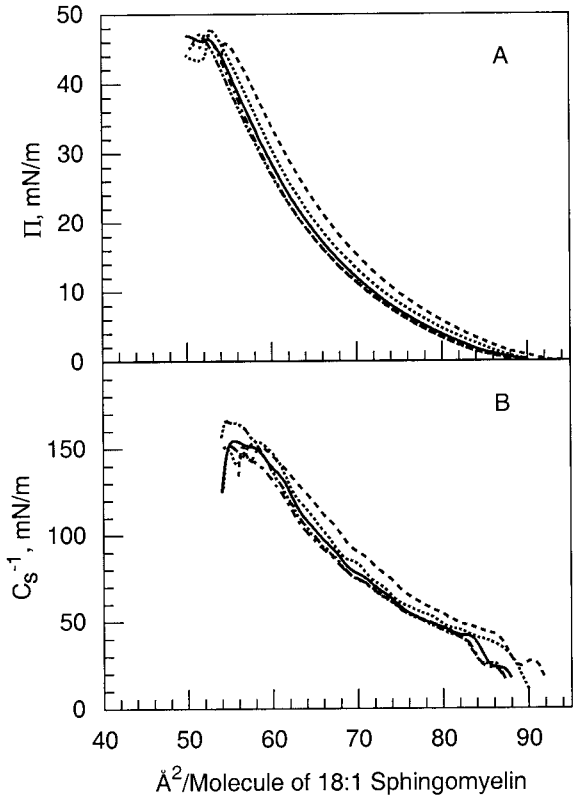

FIGURE 7 18:1 SM monolayers. (*A*) Surface pressure versus average cross-sectional molecular area (π-*A*). (*B*) Interfacial elastic modulus of area compressibility ($\mathbf{C}_s^{-1}$) versus average molecular area (other details same as in Fig. 1 legend).

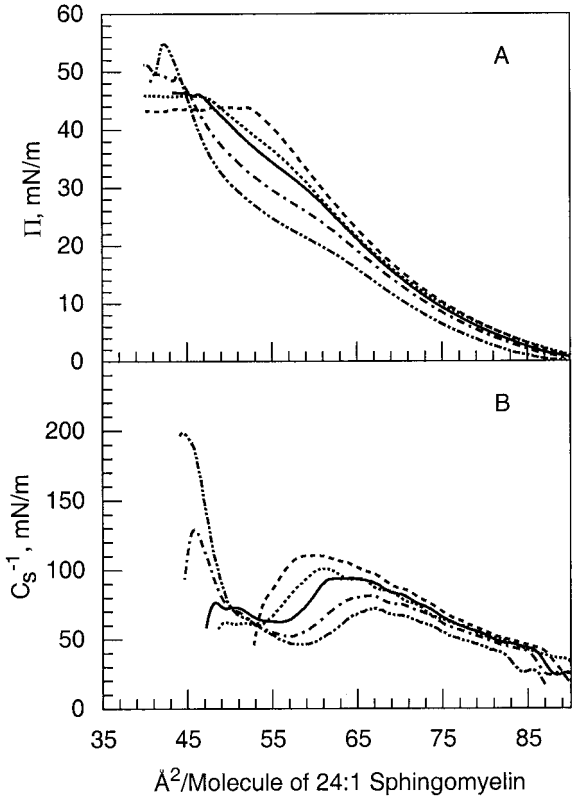

FIGURE 8 24:1 SM monolayers. (*A*) Surface pressure versus average cross-sectional molecular area (π-*A*). (*B*) Interfacial elastic modulus of area compressibility ($\mathbf{C}_s^{-1}$) versus average molecular area (other details same as in Fig. 1 legend).

1999). Transbilayer interdigitation of the chain-length asymmetric sphingolipid often is not responsible for observed differences (Almeida et al., 1992). To determine the changes in SM interfacial behavior brought about by very long saturated acyl chains relative to other acyl structural changes and in the absence of transbilayer interdigitation, we carried out the present comprehensive monolayer study of SMs with eight different acyl structures using an automated Langmuir film balance with several technical features that enhance reproducibility (see Materials and Methods). Our results clearly show that changing acyl composition and temperature affect three basic aspects of in-plane behavior: 1) two-dimensional phase transitions; 2) in-plane elasticity; 3) ability to spread.

SM two-dimensional phase transitions

In nature, saturated acyl chains with 16, 18, or 24 carbons generally dominate SM acyl composition. Our results clearly show that reducing the length of the saturated acyl chain to 14 or 12 carbons dramatically alters that two-dimensional phase behavior compared to SMs with longer saturated acyl chains. Upon reaching 16 carbons in length, further increases have marginal impact on the two-dimensional phase transition behavior with respect to the transition onset pressure. This is illustrated quantitatively by comparing the lowest temperature (T_0) at which a lipid exhibits a two-dimensional phase transition, determined from plots of the surface phase transition onset pressures versus temperature (Kellner et al., 1978). Extrapolation to the *x*-intercept provides a characteristic T_0 value for each SM (Fig. 9). In general, the lower the T_0 value, then the weaker are the intermolecular forces that stabilize the monolayers. Inspection of T_0 values (Table 3) reveals the following: SMs with saturated acyl chains of 18, 24, or 26 carbons have very similar T_0 values (18–19°C) and that of 16:0 SM is only 5–6°C lower and relatively close to the published value for DPPC (Kellner et al., 1978). Yet the T_0 value of 14:0 SM is lower by 15–20°C. These results are not entirely unexpected, given earlier SM thermotropic studies (Cohen et al., 1984; Sripada et al., 1987) which revealed that changing SM's acyl chain length (16:0, 18:0, or 24:0) has only modest impact on transition temperature. This behavior has been partially attributed to the stabilization provided by SM's ability to both donate and accept hydrogen bonds (Barenholz and Thompson, 1980; Boggs, 1987). Yet, comparison does reveal differences of monolayer T_0 and bilayer T_m values (Table 3). Note that the bilayer T_m

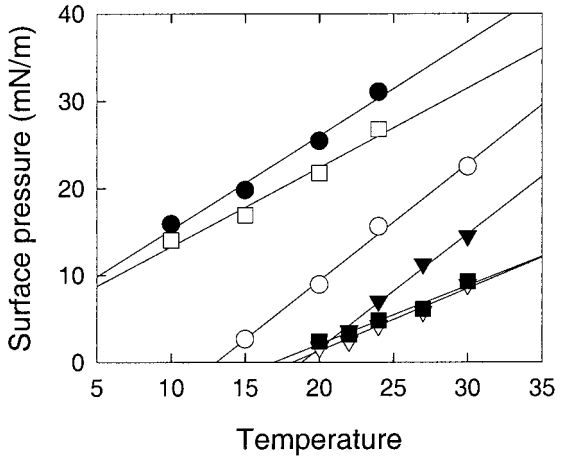

FIGURE 9 SM transition onset pressures versus temperature. Values were determined as described by Kellner et al. (1978). 14:0 SM, ●; 24:1 SM, □; 16:0 SM, ○; 18:0 SM, ▼; 24:0 SM, ▽; 26:0, ■.

values do show a definite upward trend with increasing acyl chain length that is not seen in the monolayer T_0 values for 18:0, 24:0, and 26:0 SM. This difference probably reflects the net effect that chain interdigitation has on producing increasingly thicker, more stable, bilayer gel phases for these SMs (McIntosh et al., 1992); whereas, in monolayers, no such interdigitation can occur.

In general, the existence of two-dimensional phase transitions in the 10–30°C range for 16:0 SM, 18:0 SM, and 24:0 SM sharply contrasts the behavior of another simple sphingolipid, galactosylceramide (GalCer), which shows only condensed, chain-ordered behavior over the 10–30°C temperature range when homogeneously acylated with palmitate or stearate (Ali et al., 1993, 1994). This behavior is consistent with the phosphorylcholine headgroup of SM being bulkier and more highly hydrated (by virtue of being zwitterionic) than the galactose headgroup of GalCer.

Introducing a single *cis* double bond into the 15 position of the 24-carbon acyl chain is similar to reducing the saturated acyl chain length to 14 carbons with regard to the resulting T_0 (−4.6°C vs. −4.1°C, respectively) and T_m values (Table 3). The behavior of 24:1 SM is noteworthy because this is the most common unsaturated SM species, accounting for 20–25% of the SM in bovine brain and HL-60 cells (Boegheim et al., 1983; Fitzgerald et al., 1995). Also, changing levels of 24:1 SM have been linked to central nervous system developmental processes such as myelin maturation (Babin et al., 1993) attesting to the physiological importance of acyl compositional changes in SMs. Structurally, having a *cis* double bond located between carbons 15 and 16 is expected to result in a "kink" close to the air/hydrocarbon interface where disruptions in chain-chain interactions will occur near the terminal methyl region of the adjacent sphingoid bases and diminish chain packing density (e.g., see Kulkarni and Brown, 1998). Also, it may be that the "kink" facilitates a "looping back" of the acyl chain in 24:1 to the hydrocarbon surface in ways that destabilize the monolayer and lower the resulting T_0 relative to 24:0 SM. Additional studies will be required to definitively resolve this issue.

TABLE 3 Phase characteristics

Lipid	$d\pi/dT$	T_0 (°C)	T_m (°C)
14:0 SM	1.08	−4.1	25.4
16:0 SM	1.35	13.0	40.5
18:0 SM	1.32	18.8	44.7
24:0 SM	0.72	18.2	47.1
26:0 SM*	0.67	16.9	53.6
$24:1^{\Delta 15(c)}$ SM	0.91	−4.6	26.2
di-16:0 PC†	1.71*	15.2*	41.5
di-16:0 PE†	1.42*	32.9*	63
di-14:0 PC‡	1.26	−4.3	23.8

Values for $d\pi/dT$ and T_0 (°C) were calculated from the slopes and x-intercepts, respectively, of the best fit lines to the phase transition onset surface pressure versus temperature plots (Kellner et al., 1978). The phase transition onset surface pressures were determined from the $\mathbf{C}_s^{-1}$-A plots shown in Figs. 1–8.

*T_m for 26:0 SM was determined by differential scanning calorimetry as described by Kulkarni and Brown (1998). The endotherm displayed a single peak with a transition enthalpy of ~13.4 kcal/mol.

†Monolayer values taken from Kellner et al. (1978).

‡Monolayer values for DMPC were calculated from Ali et al. (1998). T_m for the sphingolipids represent averages of values tabulated by Koynova and Caffrey (1995).

In-plane elasticity

Our data indicate that changes in the acyl composition of SMs markedly affect their in-plane elasticity. Table 2 shows that, under fluid-phase conditions, SMs with short saturated acyl chains (e.g., 12:0 or 14:0) are less elastic (in an in-plane sense) than similarly structured PCs (e.g., 14:0). This difference is likely to be a consequence of SM's capacity to hydrogen-bond with neighboring SMs. Also, SM fluid-phase $\mathbf{C}_s^{-1}$ values are relatively constant over the 10–30°C temperature range (Table 1), as has been observed with fluid-phase PCs (Ali et al., 1998). These comparisons of $\mathbf{C}_s^{-1}$ values were carried out at 30 mN/m so as to mimic membrane-like conditions. Although there is debate regarding the precise surface pressure value that places monolayers and bilayers in equilibrium (for reviews, see Marsh, 1996; MacDonald, 1996), there is agreement that high surface pressures ($\pi > 30$ mN/m) more closely mimic the bilayer situation. Comparing monolayer and bilayer in-plane elasticity values for pure SMs is not yet possible. Due to experimental challenges linked to bilayer vesicle stability below T_m, bulk compressibility moduli from membrane area dilation measurements by micropipette aspiration have only been reported for mixtures of BSM or 24:0 SM with cholesterol and not for pure SMs (Needham and Nunn, 1990; McIntosh et al., 1992). $\mathbf{C}_s^{-1}$ determinations for SMs have not yet been reported using recently developed NMR ap-

proaches (Koenig et al., 1997) or by combined x-ray diffraction and absolute specific volume measurements (Petrache et al., 1998). Yet, with lipids where comparisons are possible, the monolayer and bilayer values generally show similar trends with respect to the magnitude of change induced by alterations in lipid structure or composition (Smaby et al., 1997).

As expected at temperatures and/or surface pressures producing condensed, chain-ordered SMs, 3–3.5-fold elevations in the $\mathbf{C}_s^{-1}$ values result relative to the fluid liquid-expanded state. These $\mathbf{C}_s^{-1}$ values for the condensed SMs are higher (25–30%) than those of condensed PCs (Ali et al., 1998). A pattern is observed for each SM species showing condensed phase behavior in that the highest $\mathbf{C}_s^{-1}$ value is obtained at the lowest temperature (10°C). Also, at equivalent temperatures, condensed-phase SMs with longer acyl chains have higher $\mathbf{C}_s^{-1}$ values, consistent with enhanced van der Waals interactions achieved in the chain-ordered state. Admittedly, the absolute $\mathbf{C}_s^{-1}$ values for the condensed phase PCs and SMs must be viewed with caution. It is possible that "true equilibrium" is not attained in the monolayer condensed phases (e.g., Phillips and Hauser, 1974). Even in bilayer assemblies, simple sphingolipids are known to form various metastable gel-like phases (Bruzik et al., 1990). Nonetheless, because each lipid species was subjected to identical monolayer conditions, the relative differences do provide insights that ultimately reflect the structural differences of the various lipids.

Temperature-induced changes in spreading

A third physical feature affected by the acyl composition of SMs is their monolayer spreading behavior. Spreading of SMs with very long saturated acyl chains at temperatures 30–35° below T_m results in condensed films with lower in-plane elasticities but with consistently larger cross-sectional molecular areas than the condensed phases achieved by spreading at temperatures only 10–20° below T_m. One possible explanation for this interesting behavior is that SM spreading at the low temperatures results in relatively fast formation of rigid SM islands or surface clusters independent of the initial excess surface area at the air-water interface and of subsequent barrier compression. The ensuing compression by the barrier would simply drive the SM clusters together. However, because of their rigid, highly ordered, and possibly tilted chains, the SM clusters do not fully anneal. This results in small amounts of space becoming trapped among the rigid islands, leading to slightly larger than expected average molecular cross-sectional areas as the films approach collapse. In contrast, by spreading at temperatures sufficiently high to promote effective dispersal at excess surface area, the SM phase transition is driven by barrier compression. By passing through a liquid-expanded state, the SM molecules can translationally diffuse rapidly, resulting in more efficient (or complete) annealing with the growing condensed-phase clusters during slow barrier compression. Further experiments will be needed to test this explanation. Differences in chain tilt between low temperature-induced and barrier-produced condensed phases may also contribute to the observed differences. There is abundant evidence indicating that condensed monolayer lipid phases can exist in chain-tilted or chain-untilted forms (for review, see Kaganer et al., 1999).

Implications

Acyl saturation combined with the ability to both donate and accept hydrogen bonds appears to play a major role in endowing SMs with their physical and biological properties. In this regard, SMs are distinctly different from typical membrane PCs, which can only act as hydrogen bond donor/acceptors and have saturated *sn*-1 chains and unsaturated *sn*-2 chains. Such properties may provide SMs with enhanced tendencies to form microdomains or "lipid rafts."

A common approach used to isolate sphingolipid "rafts" from biomembranes relies on treatment of cells with 1% Triton X-100 at 4°C for 30 min (Brown and Rose, 1992; Brown, 1998). However, treatments carried out at 37°C sometimes fail to yield the detergent resistant "rafts," suggesting a low temperature-induced change in the size or physical features of the resulting "rafts." This behavior has been attributed to low temperatures facilitating a coalescence of small, but pre-existing, microdomains in biomembranes. Based on the temperature effects that we observe in monolayer behavior, the ability of the SMs to disperse, i.e., spread, depends critically on the acyl chain structure. SMs with marked acyl chain asymmetry appear to be particularly responsive to temperature-induced lateral rearrangements. In this regard, our data suggest that acyl composition may be more important than previously presumed from earlier studies of SM thermotropic behavior.

We thank Lisa Lovring for synthesizing and purifying certain of the SM derivatives.

This work was supported by USPHS Grant GM45928 (to R.E.B.) and the Hormel Foundation. The automated Langmuir film balance used in this study received major support from USPHS Grants HL49180 and HL17371 (to H.L.B.).

REFERENCES

Ahmed, S. N., D. A. Brown, and E. London. 1997. On the origin of sphingolipid/cholesterol-rich detergent-insoluble cell membranes: physiologic concentrations of cholesterol and sphingolipids induce formation of a detergent-insoluble, liquid-ordered lipid phase in model membranes. *Biochemistry.* 36:10944–10953.

Ali, S., J. M. Smaby, and R. E. Brown. 1993. Acyl structure regulates galactosylceramide's interfacial interactions. *Biochemistry.* 32: 11696–11703.

Ali, S., J. M. Smaby, and R. E. Brown. 1994. Galactosylceramides with homogeneous acyl chains: the effect of acyl structure on intermolecular

interactions occurring at the argon/buffered saline interface. *Thin Solid Films.* 244:860–864.

Ali, S., J. M. Smaby, M. M. Momsen, H. L. Brockman, and R. E. Brown. 1998. Acyl chain-length asymmetry alters the interfacial elastic interactions of phosphatidylcholines. *Biophys. J.* 74:338–348.

Almeida, P. F. F., W. L. C. Vaz, and T. E. Thompson. 1992. Lateral diffusion and percolation in two-phase, two-component bilayers. Topology of the solid-phase domains in-plane and across the lipid bilayer. *Biochemistry.* 31:7198–7210.

Babin, F., P. Sarda, B. Limasset, B. Decscomps, D. Rieu, F. Mendy, and A. Crastes de Paulet. 1993. Nervonic acid in red blood cell sphingomyelin in premature infants: an index of myelin maturation. *Lipids.* 28: 627–630.

Bar, L. K., Y. Barenholz, and T. E. Thompson. 1997. Effect of sphingomyelin composition on the phase structure of phosphatidylcholine-sphingomyelin bilayers. *Biochemistry.* 36:2507–2516.

Barenholz, Y., and T. E. Thompson. 1980. Sphingomyelins in bilayers and biological membranes. *Biochim. Biophys. Acta.* 604:129–158.

Bartlett, G. R. 1959. Phosphorus assay in column chromatography. *J. Biol. Chem.* 234:466–468.

Behroozi, F. 1996. Theory of elasticity in two dimensions and its application to Langmuir-Blodgett films. *Langmuir.* 12:2289–2291.

Bittman, R., C. R. Kasireddy, P. Mattjus, and J. P. Slotte. 1994. Interaction of cholesterol with sphingomyelin monolayers and vesicles. *Biochemistry.* 33:11776–11781.

Boegheim, J. P. J., M. van Linde, J. A. F. op den Kamp, and B. Roelofsen. 1983. The sphingomyelin pools in the outer and inner layer of the human erythrocyte membrane are composed of different molecular species. *Biochim. Biophys. Acta.* 735:438–442.

Boggs, J. M. 1987. Lipid intermolecular hydrogen bonding: influence on structural organization and membrane function. *Biochim. Biophys. Acta.* 906:353–404.

Bretscher, M. S., and S. Munro. 1993. Cholesterol and the Golgi apparatus. *Science.* 261:1280–1281.

Brockman, H. L., C. M. Jones, C. J. Schwebke, J. M. Smaby, and D. E. Jarvis. 1980. Application of a microcomputer-controlled film balance system to collection and analysis of data from mixed monolayers. *J. Colloid Interface Sci.* 78:502–512.

Brockman, H. L., J. M. Smaby, and D. E. Jarvis. 1984. Automation of surface cleaning and sample addition for surface balances. *J. Phys. E.: Sci. Instrum.* 17:351–353.

Brown, R. E. 1998. Sphingolipid organization in biomembranes: what physical studies of model membranes reveal. *J. Cell Sci.* 111:1–9.

Brown, D. A., and E. London. 1998. Functions of lipid rafts in biological membranes. *Annu. Rev. Cell Devel. Biol.* 14:111–136.

Brown, D. A., and J. K. Rose. 1992. Sorting of GPI-anchored proteins to glycolipid-enriched membrane subdomains during transport to the apical cell surface. *Cell.* 68:533–544.

Bruzik, K. S., B. Sobon, and G. M. Salamonczyk. 1990. Nuclear magnetic resonance study of sphingomyelin bilayers. *Biochemistry.* 29: 4017–4021.

Cohen, R., Y. Barenholz, S. Gatt, and A. Dagan. 1984. Preparation and characterization of well defined D-erythro sphingomyelins. *Chem. Phys. Lipids.* 35:371–384.

Davies, J. T., and E. K. Rideal. 1963. Interfacial Phenomena, 2nd. Ed. Academic Press, New York. 265.

Evans, E., and D. Needham. 1987. Physical properties of surfactant bilayer membranes: thermal transitions, elasticity, rigidity, cohesion, and colloidal interactions. *J. Phys. Chem.* 91:4219–4228.

Feng, S.-S. 1999. Interpretation of mechanochemical properties of lipid bilayer vesicles from the equation of state or pressure-area measurement of the monolayer at the air-water or oil-water interface. *Langmuir.* 15:998–1010.

Feng, S.-S., H. L. Brockman, and R. C. MacDonald. 1994. On osmotic-type equations of state for liquid-expanded monolayers of lipids at the air-water interface. *Langmuir.* 10:3188–3194.

Fitzgerald, V., M. L. Blank, and F. Snyder. 1995. Molecular species of sphingomyelin in sphingomyelinase-sensitive and sphingomyelinase-resistant pools of HL-60 cells. *Lipids.* 30:805–809.

Fornés, J. A., and J. Procopio. 1995. Density fluctuations in lipid monolayers and their possible relevance to the formation of conductive defects in bilayers. *Langmuir.* 11:3943–3947.

Gronberg, L., Z. S. Ruan, R. Bittman, and J. P. Slotte. 1991. Interaction of cholesterol with synthetic sphingomyelin derivatives in mixed monolayers. *Biochemistry.* 30:10746–10754.

Kaganer, V. M., H. Möhwald, and P. Dutta. 1999. Structure and phase transitions in Langmuir monolayers. *Rev. Mod. Phys.* 71:779–819.

Kellner, B. M. J., F. Müller-Landau, and D. A. Cadenhead. 1978. The temperature-dependence characterization of insoluble films at the air-water interface. *J. Colloid Interface Sci.* 66:597–601.

Koenig, B. W., H. H. Strey, and K. Gawrisch. 1997. Membrane lateral compressibility determined by NMR and x-ray diffraction: effect of acyl chain polyunsaturation. *Biophys. J.* 73:1954–1966.

Koynova, R., and M. C. Caffrey. 1995. Phase and phase transitions of the sphingolipids. *Biochim. Biophys. Acta.* 1255:213–236.

Kulkarni, V. S., and R. E. Brown. 1998. Thermotropic behavior of galactosylceramides with *cis*-monoenoic fatty acyl chains. *Biochim. Biophys. Acta.* 1372:347–358.

Lund-Katz, S., H. M. Laboda, L. R. McClean, and M. C. Phillips. 1988. Influence of molecular packing and phospholipid type on the rates of cholesterol exchange. *Biochemistry.* 27:3416–3423.

MacDonald, R. C. 1996. The relationship and interactions between lipid bilayer vesicles and lipid monolayers at the air/water interface. *In* Vesicles. M. Rosoff, editor. Marcel Dekker, New York, NY. 3–48.

Marsh, D. 1996. Lateral pressure in membranes. *Biochim. Biophys. Acta.* 1286:183–223.

Maulik, P. R., D. Atkinson, and G. G. Shipley. 1986. X-ray scattering of vesicles of N-acyl sphingomyelins. Determination of bilayer thickness. *Biophys. J.* 50:1071–1077.

McIntosh, T. J., S. A. Simon, D. Needham, and C. Huang. 1992. Structure and cohesive properties of sphingomyelin/cholesterol bilayers. *Biochemistry.* 31:2012–2020.

Momsen, W. E., J. M. Smaby, and H. L. Brockman. 1990. The suitability of nichrome for measurement of gas-liquid interfacial tension by the Wilhelmy method. *J. Colloid Interface Sci.* 135:547–552.

Mouritsen, O. G., J. H. Ipsen, and M. J. Zuckermann. 1989. Lateral density fluctuations in the chain-melting phase transition of lipid monolayers. *J. Colloid Interface Sci.* 129:32–40.

Nagle, J. F., and H. L. Scott. 1978. Lateral compressibility of lipid mono- and bilayers: theory of membrane permeability. *Biochim. Biophys. Acta.* 513:236–243.

Needham, D., and R. S. Nunn. 1990. Elastic deformation and failure of lipid bilayer membranes containing cholesterol. *Biophys. J.* 58: 997–1009.

Petrache, H. I., S. Tristam-Nagle, and J. F. Nagle. 1998. Fluid phase structure of EPC and DMPC bilayers. *Chem. Phys. Lipids.* 95:83–94.

Phillips, M. C., D. E. Graham, and H. Hauser. 1975. Lateral compressibility and penetration into phospholipid monolayers and bilayer membranes. *Nature.* 254:154–155.

Phillips, M. C., and H. Hauser. 1974. Spreading of solid glycerides and phospholipids at the air-water interface. *J. Colloid Interface Sci.* 49: 31–39.

Ramstedt, B., and J. P. Slotte. 1999. Interaction of cholesterol with sphingomyelins and acyl-chain-matched phosphatidylcholines: a comparative study of the effect of the chain length, *Biophys. J.* 76:908–915.

Rietveld, A., and K. Simons. 1998. The differential miscibility of lipids as the basis for the formation of functional membrane rafts. *Biochim. Biophys. Acta.* 1376:467–479.

Sankaram, M. B., and T. E. Thompson. 1990. Interactions of cholesterol with various glycerophospholipids and sphingomyelin. *Biochemistry.* 29:10670–10675.

Schroeder, R., E. London, and D. A. Brown. 1994. Interactions between saturated acyl chains confer detergent resistance on lipids and glyco-

sylphosphatidylinositol (GPI)-anchored proteins. *Proc. Natl. Acad. Sci. USA.* 91:12130–12134.

Silvius, J. R. 1992. Cholesterol modulation of lipid intermixing in phospholipid and glycosphingolipid mixtures. Evaluation using fluorescent lipid probes and brominated lipid quenchers. *Biochemistry.* 31: 3398–3408.

Silvius, J. R., D. del Guidice, and M. Lafleur. 1996. Cholesterol at different bilayer concentrations can promote or antagonize lateral segregation of phospholipids of differing acyl chain length. *Biochemistry.* 35: 15198–15208.

Simons, K., and E. Ikonen. 1997. Functional rafts in cell membranes. *Nature.* 387:569–572.

Smaby, J. M., and H. L. Brockman. 1990. Surface dipole moments of lipids at the argon-water interface. Similarities among glycerol-ester-based lipids. *Biophys. J.* 58:195–204.

Smaby, J. M., and H. L. Brockman. 1991a. A simple method for estimating surfactant impurities in solvents and subphases used for monolayer studies. *Chem. Phys. Lipids.* 58:249–252.

Smaby, J. M., and H. L. Brockman. 1991b. Evaluation of models for surface pressure-area behavior of liquid-expanded monolayers. *Langmuir.* 7:1031–1034.

Smaby, J. M., and H. L. Brockman. 1992. Characterization of lipid miscibility in liquid-expanded monolayers at the gas-liquid interface. *Langmuir.* 8:563–570.

Smaby, J. M., H. L. Brockman, and R. E. Brown. 1994. Cholesterol's interfacial interactions with sphingomyelins and phosphatidylcholines: hydrocarbon chain structure determines the magnitude of condensation. *Biochemistry.* 33:9135–9142.

Smaby, J. M., V. S. Kulkarni, M. Momsen, and R. E. Brown. 1996. The interfacial elastic packing interactions of galactosylceramides, sphingomyelins, and phosphatidylcholines. *Biophys. J.* 70:868–877.

Smaby, J. M., M. Momsen, H. L. Brockman, and R. E. Brown. 1997a. Phosphatidylcholine acyl unsaturation modulates the decrease in interfacial elasticity induced by cholesterol. *Biophys. J.* 73:1492–1505.

Smaby, J. M., M. M. Momsen, H. L. Brockman, and R. E. Brown. 1997b. The interfacial interactions of sphingomyelins with saturated acyl chains. *Biophys. J.* 72:A304.

Snyder, B., and E. Freire. 1980. Compositional domain structure in phosphatidylcholine-cholesterol and sphingomyelin-cholesterol bilayers. *Proc. Natl. Acad. Sci. USA.* 77:4055–4059.

Sripada, P. K., P. R. Maulik, J. A. Hamilton, and G. G. Shipley. 1987. Partial synthesis and properties of a series of n-acyl sphingomyelins. *J. Lipid Res.* 28:710–718.

Yedgar, S., R. Cohen, S. Gatt, and Y. Barenholz. 1982. Hydrolysis of monomolecular films of synthetic sphingomyelins by sphingomyelinase of *Staphylococcus aureus. Biochem. J.* 201:597–603.